PREPRINT: IEEE TRANSACTIONS ON AEROSPACE AND ELECTRONIC SYSTEMS, VOL. 57, NO. 4, PP. 2082-2092, JUL. 2021. DOI: 10.1109/TAES.2021.3098130

A formulation of adversarial risk for multi-object filtering

Alexey Narykov, Emmanuel Delande, and Daniel E. Clark *Senior Member, IEEE*

***Abstract*—This article is focused on estimating a quantity of interest in the context of military impact assessment that we shall call adversarial risk. We formulate adversarial risk as a function of the multi-object state describing a group of weapons, and propose two approaches to estimating it using multi-object filters. The first, optimal, approach is tailored to filters for point processes, and produces the mean estimate of adversarial risk and its variance. The second, naïve, approach is applicable to any filter producing point estimates of the multi-object state, yet it is not capable of equipping a risk estimate with an indicator of its quality. We develop an implementation of the optimal approach for a particular multi-object filter and compare it to the naïve approach.**

***Index Terms*—Impact assessment, multi-object filtering, adversarial risk**

I. Introduction

Impact assessment is an important part of military command and control. It concerns evaluation of the potential outcomes resulting from both one's own and an adversary's actions [1, p. 55]. The ability to predict impacts is useful in planning one's own actions to promote the survivability of assets [2] or to reduce the expected damage or associated costs [3]. A few available models of expected damage, such as averted harm [4, p. 58], [5, p. 7], operational risk [6, p. 52] and surviving value [7, p. 49], are useful for off-line analysis. These models address situations when actions take place on both sides, what requires modelling of complex interaction of own weapons with adversaries of varying kind, as well as solving the problem of weapon-to-target assignment [7].

The first contribution of this paper is to propose a notion of *adversarial risk* to introduce elements of impact assessment into online analysis and to describe incoming threats using streamed sensor data. Such threats could include, for example, a co-ordinated missile strike with multiple missiles [8]. Adversarial risk focuses on the actions of adversaries *exclusively*, and is defined as the expected damage to a valuable asset from a group of weapons capable of intentional malign activity. In principle, our notion of adversarial risk generalises some models of vulnerability [9], [10], [6], by permitting that only a part of the asset's value is removed by a resultative hit, without its ultimate destruction. The risk value could be subsequently used for making decisions about one's *own* actions, e.g., how to configure countermeasures, but this is beyond the scope of this paper.

The second contribution of the paper is to introduce a notion of *stochastic adversarial risk*, in order to characterize the adversarial risk when the arriving sensor data are handled by a multi-object tracking filter. It is developed within the framework of point processes theory, and is compatible with any filter that is constructed within this methodology, e.g. [11], [12], [13], [14], and possibly extends to specific interpretations of classic algorithms, e.g., joint probabilistic data-association filter (JPDA) and multiple hypotheses tracking (MHT) [15], [16], [17].

The third contribution of the paper is to develop an *optimal estimation* of the adversarial risk in the multi-object context. It provides the mean estimate of adversarial risk, which is optimal in minimum mean squared error (MMSE) sense, as well as its variance. The variance can serve as an indicator of the output's reliability, as desired by military decision makers [18], or of confidence, as expected for data fusion systems [1, Ch. 3]. Furthermore, its expressions are useful in formulation of Bayes-optimal sensor management, where the expected variance value is minimized [19], [20] or kept within constraints [21], [22], [23]. This approach is illustrated via an application to a point process intensity, or probability hypothesis density (PHD), filter [11], [12].

Section II introduces the model of adversarial risk. In Section III, we provide a description of point processes and the associated statistical tools relevant to the context of this paper. Section IV introduces stochastic adversarial risk, when the population of weapons is uncertain and described by a point process, and proposes an optimal approach to its estimation. Section V illustrates the optimal approach in the context of multi-object tracking, where the population of weapons is estimated through a Bayesian filter. Section VI demonstrates the algorithms.

II. Adversarial risk

This section develops a model of adversarial risk to characterize a multi-object population. It requires that a valuable asset is introduced to the scenario, and the population represents a group of weapons. Section II-A models the probability that an individual weapon hits the asset, Section II-B aggregates individual probabilities into the multi-object adversarial risk, Section II-C offers an illustrative example, and Section II-D

Alexey Narykov is with the Department of Electrical Engineering and Electronics at the University of Liverpool. Email: a.narykov@liverpool.ac.uk. Emmanuel Delande is a Space Surveillance Engineer in the Space Debris Modelling and Risk Assessment Office (DSO/DV/ISL) at the Centre National d'Études Spatiales (CNES), Toulouse, France Email: emmanuel.delande@cnes.fr. Daniel Clark is with Télécom SudParis, Institut Polytechnique Paris, Mines Telecom, Évry, 91001 France. Email: daniel.clark@telecom-sudparis.eu. This work was supported by the Joint AFRL-Dstl Basic-Research Grant in Autonomous Signal Processing (AFOSR grant FA9550-19-1-7008 and Dstl Task No. 1000133068). A. Narykov was supported by the James Watt scholarship from Heriot-Watt University.

TABLE I
SCENARIO DETAILS

Weapon	Loc. (m)	Range (m)	Hit prob.	Dam.cap.
x_1	$[10, 40]^T$	42.72	0.36	500
x_2	$[20, 30]^T$	30.41	0.60	500
x_3	$[40, 40]^T$	18.02	0.83	500
x_4	$[80, 10]^T$	33.54	0.54	1000
x_5	$[85, 30]^T$	53.36	0.50	1000

develops special cases of adversarial risk that will be the main focus of the paper.

A. Single-object hit

Consider a fallible weapon, whose state is described by some state space $\mathcal{X}$, to be detailed later, deemed as a possible threat for some asset A. The probability that a weapon with state $x \in \mathcal{X}$ hits the asset is described by the Bernoulli random variable $\mathrm{H}_A(x)$ with parameter $0 \leq \tau_A(x) \leq 1$, i.e., the asset is hit with probability $\tau_A(x)$. If the hit leads to the asset's destruction, which is not generally the case, the function $\tau_A(\cdot)$ simply represents the weapon's lethality [6, p. 53]. Furthermore, $\tau_A(\cdot)$ may additionally reflect various aspects of threat, such as intent and capability [24], [25]. An illustrative example will be given in Section II-C, and a more developed scenario in Section VI.

B. Multi-object adversarial risk

We assume that the asset of interest has some initial value $V_A > 0$, diminishing upon successful hits from the weapons.[1] The potential damage of a weapon with state $x \in \mathcal{X}$ is described by the random variable

$$\mathrm{D}_A(x) := d_A(x)\mathrm{H}_A(x), \tag{1}$$

where the function $d_A : \mathcal{X} \to \mathbb{R}^+$ assesses the damaging capacity of the weapon, and characterizes its ability to subtract the asset's value.

The *adversarial risk* of a group of n weapons, $n \in \mathbb{N}$, whose states are described by the sequence $x_{1:n} \in \mathcal{X}^n$ is their expected damage given by

$$\mathcal{R}_A(x_{1:n}) := \mathbb{E}\left[\min\left(V_A, \sum_{1\leq i\leq n} \mathrm{D}_A(x_i)\right)\right]. \tag{2}$$

This model captures the fact that the weapons cannot inflict damage that is bigger than the value of the asset itself.

C. Illustrative example

We study the adversarial risk (2) with a focus on the interaction between the damaging capacities of weapons and the asset's diminishing value, which are novel in this model.

[1]The idea of modelling the asset's value as diminishing gradually (rather than disappearing following a single strike) is inspired by the models of expected damage, which are focused on a set of dispersed assets whose total value is computed as the sum of individual values and it is permitted that only a subset of assets survives an attack [6], [7]. The asset of diminishing value can be seen as an evolution of that model provided that the assets are concentrated in a single location. In practice, the value of an asset is a complex matter to which many different aspects contribute [6, p. 54]

The state space $\mathcal{X}$ describes here the coordinates of a weapon in the 2D state space (see Figure 1a). We consider a population of five weapons with states x_i, $1 \leq i \leq 5$, as given in Table I. In this particular case, the valuable asset is also described by its coordinates $x_A = [50, 25]^T\mathrm{m}$ in the 2D plane. The hit probability is then modelled with a Gaussian function [9], i.e.,

$$\tau_A(x) := \exp\left(-\frac{r(x, x_A)^2}{2b_r^2}\right), \tag{3}$$

where $r : \mathcal{X} \times \mathcal{X} \to \mathbb{R}^+$ evaluates the distance, and $b_r > 0$ is a parameter describing the spread of the potential hit. Its shape is presented in Figure 1a for $b_r = 30\mathrm{m}$.

The damaging capacity of the weapon is assumed to depend on whether the adversary is sea-based or land-based, that is,

$$d_A(x) := \begin{cases} 1000 & \text{if } x \in B \text{ (sea-based)}, \\ 500 & \text{if } x \in \bar{B} \text{ (land-based)}. \end{cases} \tag{4}$$

The corresponding ranges as well as the resulting hit probabilities and damaging capacities for the considered weapons are in Table I. Note that the specific choice of functions (3) and (4), and their dependencies on the scenario geometry is only for demonstration purposes. Other functions can be used as deemed appropriate, e.g. [26, Eq. (34)], [27, Sec. 5], [28, Eq. (4)].

Figure 1c evaluates adversarial risk (2) over a range of possible asset values $V_A \in [0, 8000]$. When the asset value is higher than the damaging capacity of all weapons combined ($V_A \geq 3500$), i.e., *the asset value is very high*, the risk value is independent of variation in V_A. When the asset value is lower than the lowest damaging capacity ($V_A \leq 500$), i.e., *the damaging capacity of each weapon is very high*, the risk value is proportional to V_A. These observations motivate the developments in Section II-D.

Figure 2 offers a visualisation of risk maps for the two critical asset values. The maps of this kind are a valuable decision-making aid in route planning, e.g., [3], [29], [28].

D. Limiting cases of adversarial risk

We shall focus, for the rest of the paper, on two special cases where the adversarial risk has a simpler structure than (2). Despite obtained from idealised assumptions, those limiting cases represent practically significant quantities.

Assumptions II.1 (Infinite asset value)**.** *The damage function $d_A(\cdot)$ is finite-valued, while the asset value is infinite, i.e.,*

$$V_A = +\infty. \tag{5}$$

The principal consequence of this assumption is that the asset can take any number of hits and any amount of damage without losing its total value. Thus, the risk evaluates to the full damage expected from a group of fallible weapons with finite damaging capacities.

Proposition II.2 (Σ-risk)**.** *Under Assumptions II.1, the adversarial risk* (2) *simplifies as*

$$\mathcal{R}_{A,\Sigma}(x_{1:n}) = \sum_{1\leq i\leq n} d_A(x_i)\tau_A(x_i), \tag{6}$$

for a population of weapons with states $x_{1:n} \in \mathcal{X}^n$.

The proof is given in Appendix A-A. It is worth noting that the model (6) offers a physically meaningful interpretation of 'cumulative threat' which is a quantity defined additive across the weapons, e.g., [30], [29], [31].

Assumptions II.3 (Infinite damaging capacity)**.** *The damaging capacity of weapons is infinite, i.e.,*

$$\forall x \in \mathcal{X}, \quad d_A(x) = +\infty, \tag{7}$$

while the asset value V_A *is finite.*

This implies that the asset loses its total value following a single strike from a weapon. As a result, the risk evaluates to the asset value weighted by the probability of at least one strike from a group of weapons.

Proposition II.4 (Π-risk)**.** *Under Assumptions II.3, the adversarial risk* (2) *simplifies as*

$$\mathcal{R}_{A,\Pi}(x_{1:n}) = V_A \cdot \left[1 - \prod_{1\leq i\leq n} \left[1 - \tau_A(x_i)\right]\right], \tag{8}$$

for a population of weapons with states $x_{1:n} \in \mathcal{X}^n$.

The proof is given in Appendix A-B. The structure of (8) is compatible with other models of expected damage [4], [6], [7]. For $V = 1$, it is equivalent to the 'probability of kill' [2] or 'vulnerability' in [10, Eq. 18], and can be seen as generalisation of [9] to multiple weapons.

In the rest of the paper subscripts related to the asset may be omitted, when there is no ambiguity, for the sake of simplicity.

III. Background on point processes

This section presents background and notation used throughout the article and does not contain novel material. Point processes are briefly described in Section III-A, Section III-B introduces statistical moments to describe a point process, and Section III-C introduces the probability generating functional.

A. Point processes

In this article, the objects of interest, i.e., the weapons, have individual states x in some d_{x}-dimensional state space $\mathcal{X} \subset \mathbb{R}^{d_{\mathrm{x}}}$, typically consisting of position, velocity and class variables. A point process Φ on $\mathcal{X}$ is a random variable on the process space $\mathfrak{X} = \bigcup_{n=0}^{\infty} \mathcal{X}^n$, i.e. the space of all finite sequences of points in $\mathcal{X}$, whose number of elements *and* element states are unknown and (possibly) time-varying.[2] A realisation of Φ is a sequence $x_{1:n} \in \mathcal{X}^n$, representing a *population* of n objects with states $x_i \in \mathcal{X}$, $1 \leq i \leq n$, where $n \in \mathbb{N}$. In the context of multi-object filtering, this sequence depicts a specific multi-object configuration.

As for usual real-valued random variables, a point process is described by its probability distribution P_Φ on $\mathfrak{X}$; the projection measure $P_\Phi^{(n)}$ describes the realisations of Φ with n elements, $n \geq 0$. The projection measures are assumed to be symmetrical functions, so that the order of points in a realisation is irrelevant for statistical purposes and the permutations of a realization of the point process—such as (x_1, x_2) and (x_2, x_1)—are equally probable. In addition, a point process is called *simple* if the probability distribution is such that realisations are sequences of points that are pairwise distinct almost surely, i.e., a realization does not contain repetitions. For the rest of the paper, all the point processes are assumed simple. The density of the projection measure $P_\Phi^{(n)}$, $n \geq 0$, is then denoted by $p_\Phi^{(n)}$.

[2]More formally, a point process Φ on $\mathcal{X}$ is a measurable mapping $\Phi : (\Omega, \mathcal{F}, \mathbb{P}) \to (\mathfrak{X}, \mathcal{B}(\mathfrak{X}))$ from some probability space $(\Omega, \mathcal{F}, \mathbb{P})$ to the measurable space $(\mathfrak{X}, \mathcal{B}(\mathfrak{X}))$, where Ω is a sample space; $\mathcal{F}$ is a σ-algebra on Ω; $\mathbb{P}$ is a probability measure on $(\Omega, \mathcal{F})$; $\mathcal{B}(\mathfrak{X})$ is the Borel σ-algebra on $\mathfrak{X}$ [32].

B. Statistical moments

An alternative description of a point process Φ is through densities of its statistical moments which only carry partial information. Specifically, we focus on the lower-order moments that carry the most information. The statistics $(\mu_\Phi, \nu_\Phi^{(2)})$ of the process Φ are the first *non-factorial* moment density μ_Φ, also called *intensity*, that coincides with the first *factorial* moment density, and the second factorial moment density $\nu_\Phi^{(2)}$. The statistics are defined on $\mathcal{X}$ as

$$\mu_\Phi(x) := \sum_{n\geq 0} \int \left(\sum_{1\leq i\leq n} \delta_x(x_i) \right) p_\Phi^{(n)}(x_{1:n}) \mathrm{d}(x_{1:n}), \tag{9}$$

$$\nu_\Phi^{(2)}(x, \bar{x}) := \sum_{n\geq 0} \int \left(\sum_{1\leq i,j\leq n}^{\neq} \delta_x(x_i)\delta_{\bar{x}}(x_j) \right) p_\Phi^{(n)}(x_{1:n}) \mathrm{d}(x_{1:n}), \tag{10}$$

where δ is the Dirac delta function, i.e. such that the equality $\int \delta_y(x) f(x) \mathrm{d}x = f(y)$ holds for any function f, and the $\sum_{i,j}^{\neq}$ notation means that it is a double sum over indices i and j where $i \neq j$ [32]. These moments will be used to evaluate Σ-risk for an uncertain population of weapons.

C. Probability generating functional

It can be convenient to describe point processes with their probability generating functional (p.g.fl.) [33]. For a point process Φ, the probability generating functional is defined as an expectation

$$\mathcal{G}_\Phi(h) := \sum_{n\geq 0} \int \left[\prod_{1\leq i\leq n} h(x_i) \right] P_\Phi^{(n)}(\mathrm{d}(x_{1:n})), \tag{11}$$

where $h : \mathcal{X} \to [0, 1]$ a test function. This tool will be used to evaluate Π-risk for an uncertain population of weapons.

IV. Risk statistics for multi-object populations

In this section we establish the adversarial risk, introduced in Section II, in the context where the population of weapons is uncertain and described by some point process Φ as covered in Section III.

A. Approaches to estimation of the adversarial risk

The adversarial risk is defined in Section II for a *known* population of weapons. Given the point process Φ describing

the uncertain population of weapons, we shall consider two approaches to produce a risk estimate:

1) Extract a meaningful point estimate of the population from the point process, then evaluate the adversarial risk generated by this population estimate.
2) Describe the adversarial risk with a random variable, whose uncertainty is induced by the point process, then extract meaningful statistics about this random variable.

The first approach, which we describe as *naïve*, is an efficient, flexible solution that can accommodate a wide variety of point processes in input, as well as of risk functions to evaluate. However, it merely produces a guess about the risk value without providing any indication of its quality or whether this estimate is optimal in any sense.

We shall focus, in the rest of the paper, on the second approach. In particular, we aim to produce the *mean* and *variance* of the adversarial risk, to be drawn from the statistics of the weapon point process, so as to provide a risk estimate that is optimal in the MMSE sense.

B. Stochastic adversarial risk and its statistics

The weapon point process Φ induces a random variable in the risk space, representing the uncertainty in the adversarial risk stemming from the uncertainty in the size and composition of the population of weapons. More precisely, the *stochastic* adversarial risk is the real-valued random variable

$$\mathrm{R}_\Phi := \mathcal{R} \circ \Phi, \tag{12}$$

where $\circ$ denotes the function composition operator. The construction of the random variable is illustrated on Figure 3.

The mean $\mu_{\mathcal{R},\Phi}$ and variance $\sigma^2_{\mathcal{R},\Phi}$ of the stochastic adversarial risk can then be built upon the stochastic description of the point process Φ, and are given by

$$\mu_{\mathcal{R},\Phi} := \mathbb{E}[\mathrm{R}_\Phi] \tag{13a}$$
$$= \sum_{n\geq 0} \int \mathcal{R}(x_{1:n}) P^{(n)}_\Phi(\mathrm{d}(x_{1:n})), \tag{13b}$$

$$\sigma^2_{\mathcal{R},\Phi} := \mathbb{E}[\mathrm{R}^2_\Phi] - \mathbb{E}[\mathrm{R}_\Phi]^2 \tag{14a}$$
$$= \sum_{n\geq 0} \int \mathcal{R}(x_{1:n})^2 P^{(n)}_\Phi(\mathrm{d}(x_{1:n})) - \left[\sum_{n\geq 0} \int \mathcal{R}(x_{1:n}) P^{(n)}_\Phi(\mathrm{d}(x_{1:n}))\right]^2. \tag{14b}$$

C. Statistics of Σ-risk and Π-risk

We develop here the statistics of stochastic adversarial risk for the special cases introduced in Section II.

Theorem IV.1 (Statistics of stochastic Σ-risk)**.**
The statistics $(\mu_{\Sigma,\Phi}, \sigma^2_{\Sigma,\Phi})$ of the stochastic Σ-risk are obtained from the statistics $(\mu_\Phi, \nu^{(2)}_\Phi)$ of the weapon point process Φ as

$$\mu_{\Sigma,\Phi} = \int d(x)\tau(x)\mu_\Phi(x)\mathrm{d}x, \tag{15}$$

$$\sigma^2_{\Sigma,\Phi} = \int d(x)^2\tau(x)^2\mu_\Phi(x)\mathrm{d}x - \left(\int d(x)\tau(x)\mu_\Phi(x)\mathrm{d}x\right)^2 + \int d(x)\tau(x)d(\bar{x})\tau(\bar{x})\nu^{(2)}_\Phi(x,\bar{x})\mathrm{d}(x,\bar{x}). \tag{16}$$

The proof is given in Appendix A-C. This result first appeared in [30], and the proof is presented here for the sake of completeness.

Note that if the damage is assumed to be unitary — i.e., $d(x) = 1$ for any $x \in \mathcal{X}$ — and the probability of hitting the asset is assumed to be the indicator function in some region $B \subseteq \mathcal{X}$, i.e.,

$$\tau(x) = \begin{cases} 1, & x \in B \\ 0, & x \notin B, \end{cases} \tag{17}$$

then the statistics (15)–(16) reduce to the regional statistics [34] and simply describe the number of weapons in B. Note that 'cookie cutter' functions analogous to (17) are also employed to indicate targets of interest in [35], [36].

Theorem IV.2 (Statistics of stochastic Π-risk)**.**
The statistics $(\mu_{\Pi,\Phi}, \sigma^2_{\Pi,\Phi})$ of the stochastic Π-risk are obtained from the p.g.fl. $\mathcal{G}_\Phi$ of the weapon point process Φ as

$$\mu_{\Pi,\Phi} = V \cdot \big(1 - \mathcal{G}_\Phi[1-\tau]\big), \tag{18}$$
$$\sigma^2_{\Pi,\Phi} = V^2 \cdot \big(\mathcal{G}_\Phi[(1-\tau)^2] - \mathcal{G}_\Phi[1-\tau]^2\big) \tag{19}$$

The proof is given in Appendix A-D.

V. Application to multi-object filtering

In this section we aim to provide expressions for computing statistics of risk using densities of lower-order statistical moments and p.g.fl. extracted from a practical multi-object filter. In Section V-A, we focus on the intensity filter [11], [12] and identify the updated process from which we wish to produce statistics. Then we develop expressions for computing densities of the first and second order moments, and its p.g.fl. In Section V-B, we proceed to develop expressions for computing statistics describing adversarial risk, i.e. its mean and variance. The derivations in this section use the model and Bayesian updated p.g.fl. derived by Bakut and Ivanchuk [11], and the derivation of the variance from [34].

A. Process statistics from a practical filter

We shall assume that the population of weapons is estimated through a multi-object filter [12]. We wish here to produce the p.g.fl. (11) and statistics (9)-(10) of the filtered process following the k-th Bayesian iteration, from which we will then extract the risk statistics in Section V-B. In the k-th data update step, the predicted process $\Phi_{k|k-1}$ is updated to Φ_k given a sequence $z_{1:m} \in \mathcal{Z}^m$ of m observations, $m \geq 0$, belonging to some observation space $\mathcal{Z} \subset \mathbb{R}^{d_z}$ and collected from the sensor. This step relies on the following assumptions [11]:

Assumptions V.1.
(a) The predicted object process $\Phi_{k|k-1}$ is Poisson with intensity $\mu_{k|k-1}$.
(b) The measurements originating from object detections are generated independently from each other.

(c) An object with state $x \in \mathcal{X}$ is detected with probability $p_{\mathrm{d},k}(x)$; if so, it produces a measurement whose state is distributed according to a likelihood $g_k(\cdot|x)$.
(d) The process describing false alarms produced by the sensor is Poisson with intensity μ_k^{fa}.

For the sake of convenience we define the missed detection and association terms for any observation $z \in \mathcal{Z}$ as

$$\mu_k^{\phi}(x) = (1 - p_{\mathrm{d},k}(x))\mu_{k|k-1}(x), \tag{20}$$
$$\mu_k^{z}(x) = p_{\mathrm{d},k}(x)g_k(z|x)\mu_{k|k-1}(x), \tag{21}$$

and for an arbitrary function $f : \mathcal{X} \to \mathbb{R}^+$ we define

$$F_k^{\phi}[f] := \int f(x)\mu_k^{\phi}(x)\mathrm{d}x, \tag{22}$$
$$F_k^{z}[f] := \int f(x)\mu_k^{z}(x)\mathrm{d}x. \tag{23}$$

Proposition V.2 (Extracted process moments)**.** *Under Assumptions V.1, the statistics $\left(\mu_k, \nu_k^{(2)}\right)$ of the updated process Φ_k are given by*

$$\mu_k(x) = \mu_k^{\phi}(x) + \sum_{1\le i\le m} \frac{\mu_k^{z_i}(x)}{F_k^{z_i}[1] + \mu_k^{\mathrm{fa}}(z_i)}, \tag{24}$$

$$\begin{aligned}\nu_k^{(2)}(x,\bar{x}) =& \mu_k^{\phi}(x)\mu_k^{\phi}(\bar{x}) + \mu_k^{\phi}(x) \sum_{1\le i\le m} \frac{\mu_k^{z_i}(\bar{x})}{F_k^{z_i}[1] + \mu_k^{\mathrm{fa}}(z_i)} \\ &+\mu_k^{\phi}(\bar{x}) \sum_{1\le i\le m} \frac{\mu_k^{z_i}(x)}{F_k^{\bar{z}}[1] + \mu_k^{\mathrm{fa}}(z_i)} \\ &+ \sum_{1\le i,j\le m}^{\neq} \left(\frac{\mu_k^{z_i}(x)}{F_k^{z_i}[1] + \mu_k^{\mathrm{fa}}(z_i)}\right)\left(\frac{\mu_k^{z_j}(\bar{x})}{F_k^{z_j}[1] + \mu_k^{\mathrm{fa}}(z_j)}\right).\end{aligned} \tag{25}$$

Proof. For the considered intensity filter, the general expression of updated intensity (24) is developed in [11]. The expression of the second-order factorial moment (25) is obtained from the second-order non-factorial moment in [34, Eq. 31] using [32, Eq. 4.3.4]. □

Proposition V.3 (Extracted process p.g.fl. [11])**.** *Under Assumptions V.1, the p.g.fl. $\mathcal{G}_k$ of the updated process Φ_k is given by*

$$\mathcal{G}_k(h) = \frac{e^{F_k^{\phi}[h]}}{e^{F_k^{\phi}[1]}} \prod_{1\le i\le m} \frac{F_k^{z_i}[h] + \mu_k^{\mathrm{fa}}(z_i)}{F_k^{z_i}[1] + \mu_k^{\mathrm{fa}}(z_i)} \tag{26}$$

for a test function $h : \mathcal{X} \to [0, 1]$.

B. Risk statistics from process statistics

Assuming that a population of weapons is maintained by a multi-object filter, and described at the k-th Bayesian step by the p.g.fl. (26) and statistics (24)-(25) as detailed in Section V-A, we can now produce the statistics of the stochastic adversarial risk generated by these weapons.

Theorem V.4 (Extracted statistics of stochastic Σ-risk)**.** *Under Assumptions V.1, the statistics $(\mu_{\Sigma,k}, \sigma^2_{\Sigma,k})$ of the stochastic adversarial Σ-risk (15)–(16) are given by*

$$\mu_{\Sigma,k} = F_k^{\phi}[d\tau] + \sum_{1\le i\le m} \frac{F_k^{z}[d\tau]}{F_k^{z_i}[1] + \mu_k^{\mathrm{fa}}(z_i)}, \tag{27}$$

$$\begin{aligned}\sigma^2_{\Sigma,k} =& F_k^{\phi}[d^2\tau^2] + \sum_{1\le i\le m} \left[\frac{F_k^{z_i}[d^2\tau^2]}{F_k^{z_i}[1] + \mu_k^{\mathrm{fa}}(z_i)}\right. \\ &\left. - \left(\frac{F_k^{z_i}[d\tau]}{F_k^{z_i}[1] + \mu_k^{\mathrm{fa}}(z_i)}\right)^2\right].\end{aligned} \tag{28}$$

The expression analogous to (27) was first presented in [35], and the analog of (28) was first presented by the authors in [30]. The proof is given in Appendix A-E for the sake of completeness.

Theorem V.5 (Extracted statistics of stochastic Π-risk)**.** *Under Assumptions V.1, the statistics $(\mu_{\Pi,k}, \sigma^2_{\Pi,k})$ of the stochastic adversarial Π-risk (18)–(19) are given by*

$$\mu_{\Pi,k} = V \frac{e^{F_k^{\phi}[\tau]}}{e^{F_k^{\phi}[1]}} \prod_{1\le i\le m} \frac{F_k^{z_i}[\tau] + \mu_k^{\mathrm{fa}}(z_i)}{F_k^{z_i}[1] + \mu_k^{\mathrm{fa}}(z_i)}, \tag{29}$$

$$\begin{aligned}\sigma^2_{\Pi,k} =& V^2\left[\frac{e^{F_k^{\phi}[\tau^2]}}{e^{F_k^{\phi}[1]}} \prod_{1\le i\le m} \frac{F_k^{z_i}[\tau^2] + \mu_k^{\mathrm{fa}}(z_i)}{F_k^{z_i}[1] + \mu_k^{\mathrm{fa}}(z_i)}\right. \\ &\left. - \left(\frac{e^{F_k^{\phi}[\tau]}}{e^{F_k^{\phi}[1]}} \prod_{1\le i\le m} \frac{F_k^{z_i}[\tau] + \mu_k^{\mathrm{fa}}(z_i)}{F_k^{z_i}[1] + \mu_k^{\mathrm{fa}}(z_i)}\right)^2\right].\end{aligned} \tag{30}$$

Proof. The result follows from Theorem IV.2 using the p.g.fl. of the updated process from Proposition V.3 and by selecting the probability of hit function τ as test function. □

In the following section, we present a simulated study demonstrating a dynamic scenario with multiple weapons and introduced risk models.

VI. Simulated example

In this section we analyse the performance of estimation algorithms for a hypothetical attack scenario using synthetic data. The optimal approach is contrasted to the naïve implementation, which relies on the explicit step of state estimation. A Sequential Monte Carlo (SMC) implementation of an intensity filter [37] has been utilised.

A. Population modelling

A static range-bearing sensor located at the origin takes measurements from four weapons that appear in the surveillance area at times $[10, 20, 30, 40]$s during the scenario that lasts $50\,\mathrm{s}$. The sensor field of view (FoV) is the quadrant with radius $2500\,\mathrm{m}$. The measurements are contaminated with zero-mean Gaussian noise with standard deviation in range $5\,\mathrm{m}$, and in bearing 1°, and immersed in Poisson false alarms with rate $\lambda_{\mathrm{fa}} = 20$ and uniformly distributed over the FoV.

The state space $\mathcal{X} \subseteq \mathbb{R}^4$ describes the position and velocity coordinates of a weapon, within the 2D region covered by the sensor FoV. The weapons evolve in the sensor FoV following a near-constant velocity motion model [38], with the variance of velocity increments set to $0.25\mathrm{m}^2\mathrm{s}^{-3}$ (as depicted on Figure 4). These positions are sampled from a Gaussian spatial distribution with mean $[500, 500]^T\mathrm{m}$ and covariance with non-zero diagonal elements $50000\mathrm{m}^2$, $50000\mathrm{m}^2$, and velocities set to $10\mathrm{m\,s}^{-1}$ in the direction of the mean.

The arrival of weapons in the FoV is described in the filter with a Poisson point process with rate 0.1 and the same spatial distribution as above in the position subspace, while the absolute speed values are uniformly distributed in $[5, 15]\mathrm{m\,s^{-1}}$. The probability of survival of an individual weapon is set to 0.99.

Position ground truth over 50 time steps is displayed in Figure 4.

B. Risk modelling

The valuable asset is described by its coordinates $x_A = [500, 500]^T\mathrm{m}$ in the 2D plane. For the Σ-risk model, the damaging capacity is set to $d_A = 100$ for all weapon states. For the Π-risk model, the asset value is set to $V_A = 1$.

Each weapon is described by its hit probability τ_A. In contrast to Section II-C, we consider a more nuanced model of hit probability

$$\tau_A(x) := \mathrm{c}_A(x)\mathrm{i}_A(x), \tag{31}$$

which comprises the common threat components [25], [24] of capability $\mathrm{c}_A : \mathcal{X} \to [0, 1]$ and intent $\mathrm{i}_A : \mathcal{X} \to [0, 1]$. The capability to produce a hit is modelled similarly to (3), i.e., by a Gaussian function [9] of range with a sensitivity parameter $b_r = 86.6\,\mathrm{m}$. The intent to produce a hit is also modelled by a Gaussian function

$$\mathrm{i}_A(x) = \exp\left(-\frac{\theta(x, x_A)^2}{2b_\theta^2}\right), \tag{32}$$

where $\theta : \mathcal{X} \times \mathcal{X} \to [0, \pi]$ evaluates the angle-of-attack, i.e., the absolute deviation (in radians) between the weapon's heading and direction to the asset, and a positive sensitivity parameter is set to $b_\theta = 0.5\,\mathrm{rad}$. Figure 5 plots the threat-dominating dimensions of range and angle-of-attack, as well as the hit probability against time.

Note that the specific choice of function (32) is only for demonstration purposes, and other functions can be used, e.g., as in [39, Eq. (16)]. Finally, more involved models than (31) can be found in [24], [40], [41] and references therein.

C. Performance assessment

In Figure 6, we present the clairvoyant values (black lines) together with their estimates. These ideal values reveal the difference in behaviour of the risk models and highlight their sensitivity to the geometry formed between the adversaries and the asset. The clairvoyant risk value is computed by evaluating the definition of adversarial risk in the true multi-object state describing a group of weapons. The naïve estimate is computed similarly, but the true state is replaced by a multi-object state estimate, determined from the output of the filter.

Specifically, in the settings of Σ-risk, the risk value is obtained as a probability-weighted sum of individual damaging capacities. As a result, it clearly reflects the possible added impact of each weapon provided that the associated hit probability is high. In the settings of Π-risk, the risk value is proportional to the asset value and is obtained as the asset value weighted by the probability of at least one hit. Accordingly, once there is at least one weapon associated with a high probability of a hit, the possible added impacts of other weapons are not clearly seen.

The optimal approach obtains the risk estimation results using expressions developed in Section V-B, and those result are contrasted to the naïve approach outlined in Section IV-A. The variance in the estimated parameter, as produced by the optimal approach, is used to quantify the level of uncertainty in the mean parameter value. Specifically, we present confidence intervals as the square root of the risk variance which in turn admits a standard deviation interpretation. It is worth noting that this information is not available in the naïve approach, despite being a desirable feature indicating reliability of an estimate.

We evaluate the produced estimates by comparing them to their ideal values in order to establish whether the proposed approach offers improvements in terms of mean squared error (MSE). Figure 7 presents the MSE values for both approaches. In both approaches, the observed results are consistent with the fact that lower probability of detection results into higher uncertainty in the population, and thus leads to the higher values of resulting MSE.

Overall, the optimal approach appears to outperform the naïve implementation, since the MSE is smaller during the most of scenario. However, the naïve algorithm may offer superior performance when the value of risk falls into the extreme values, e.g., in the absence of objects or when Π-risk gets saturated. This behaviour in the naïve algorithm is due to the fact that it relies on the hard decision of extracting the system state to estimate risk, and so is likely to point precisely at the extreme situation, e.g. the absence of weapons.

Figure 8 demonstrates the values of MSE averaged over the whole length of scenario. The proposed optimal approach offers a 15-30 percent performance improvement with respect to the naïve approach. Furthermore, this improvement appears to gradually increase as the sensor's probability of detection decreases.

VII. Conclusion

We introduce in this paper the concept of adversarial risk emanating from a group of weapons. In practice, it is often not possible to establish the number and states of such weapons with certainty. This article proposed an algorithm that takes into account the uncertainty in the weapon population, represented as a point process, and produces the estimates of the risk value. We offered an implementation for a particular multi-object filter. The algorithm is verified using synthetic data for a hypothetical attack scenario. Its performance is compared to that of a naïve approach, which relies on an explicit step of multi-object state extraction prior to evaluating the risk value.

Appendix A
Proofs

A. Proof of Proposition II.2

Proof. Under Assumptions II.1, the risk in (2) is given by

$$\mathcal{R}(x_{1:n}) = \mathbb{E}\left[\sum_{1\le i\le n} \mathrm{D}_A(x_i)\right] \tag{33a}$$

$$= \sum_{1\le i\le n} \mathbb{E}[\mathrm{D}_A(x_i)] \tag{33b}$$
$$= \sum_{1\le i\le n} \mathbb{E}[d_A(x_i)\mathrm{H}_A(x_i)] \tag{33c}$$
$$= \sum_{1\le i\le n} (d_A(x_i)\cdot\tau_A(x_i) + 0\cdot[1-\tau_A(x_i)]) \tag{33d}$$
$$= \sum_{1\le i\le n} d_A(x_i)\tau_A(x_i). \tag{33e}$$

□

B. Proof of Proposition II.4

Proof. Under Assumptions II.3, the risk in (2) is given by

$$\mathcal{R}(x_{1:n}) = V_A\cdot p_1 + 0\cdot p_0 \tag{34a}$$
$$= V_A\cdot(1-p_0), \tag{34b}$$

where p_1 is the probability of at least one resultative hit, and $p_0 = 1-p_1$ is the probability of no hits given by

$$p_0 = \prod_{1\le i\le n}\left[1-\tau_A(x_i)\right]. \tag{35}$$

Substituting (35) into (34b) yields the desired result. □

C. Proof of Theorem IV.1

Proof. Let us obtain the statistics $(\mu_{\Sigma,\Phi}, \sigma^2_{\Sigma,\Phi})$ of the stochastic Σ-risk. From (13b) and (6) we can write the expected value as

$$\mu_{\Sigma,\Phi} = \sum_{n\ge 0}\int\left(\sum_{1\le i\le n} d(x_i)\tau(x_i)\right)P_\Phi^{(n)}(\mathrm{d}(x_{1:n})), \tag{36a}$$

and using Campbell's theorem [32, p. 103] then yields

$$\mu_{\Sigma,\Phi} = \int d(x)\tau(x)\mu_\Phi(x)\mathrm{d}x. \tag{36b}$$

Next we focus on the variance defined in (14a). The expected value $\mathbb{E}[\mathrm{R}^2_\Phi]$ is obtained from (13b) and (6) and written as

$$\mathbb{E}[\mathrm{R}^2_\Phi] = \sum_{n\ge 0}\int\left(\sum_{1\le i\le n} d(x_i)\tau(x_i)\right)^2 P_\Phi^{(n)}(\mathrm{d}(x_{1:n})) \tag{37a}$$
$$= \sum_{n\ge 0}\int\left(\sum_{1\le i\le n} d(x_i)^2\tau(x_i)^2\right)P_\Phi^{(n)}(\mathrm{d}(x_{1:n})) + \sum_{n\ge 0}\int\left(\sum_{1\le i,j\le n}^{\neq} d(x_i)\tau(x_i)d(x_j)\tau(x_j)\right)P_\Phi^{(n)}(\mathrm{d}(x_{1:n})) \tag{37b}$$
$$= \int d(x_i)^2\tau(x)^2\mu_\Phi(x)\mathrm{d}x + \int d(x)\tau(x)d(\bar{x})\tau(\bar{x})\nu_\Phi^{(2)}(x,\bar{x})\mathrm{d}(x,\bar{x}), \tag{37c}$$

where $\nu_\Phi^{(2)}(\cdot,\cdot)$ is defined in (10). Substituting (37c) and (36b) into (14a) yields the variance of the stochastic Σ-risk.

□

D. Proof of Theorem IV.2

Proof. Let us obtain the statistics $(\mu_{\Pi,\Phi}, \sigma^2_{\Pi,\Phi})$ of the stochastic Π-risk. From (13b) and (8) we can write the expected value

$$\mu_{\Pi,\Phi} = \sum_{n\ge 0}\int V\left[1-\prod_{1\le i\le n}\left[1-\tau(x_i)\right]\right]P_\Phi^{(n)}(\mathrm{d}(x_{1:n})) \tag{38a}$$
$$= V\left[1-\sum_{n\ge 0}\int\left[\prod_{1\le i\le n}\left[1-\tau(x_i)\right]\right]P_\Phi^{(n)}(\mathrm{d}(x_{1:n}))\right], \tag{38b}$$

then using the definition of p.g.fl. in (11) yields

$$\mu_{\Pi,\Phi} = V\cdot\big(1-\mathcal{G}_\Phi[1-\tau]\big). \tag{38c}$$

Next we focus on the variance defined in (14a). The expected value $\mathbb{E}[\mathrm{R}^2_\Phi]$ is obtained from (13b) and (8) and written as

$$\mathbb{E}[\mathrm{R}^2_\Phi] = \sum_{n\ge 0}\int\left[V\cdot\left[1-\prod_{1\le i\le n}\left[1-\tau(x_i)\right]\right]\right]^2 P_\Phi^{(n)}(\mathrm{d}(x_{1:n})) \tag{39a}$$
$$= V^2\cdot\big(1-2\mathcal{G}_\Phi[1-\tau]+\mathcal{G}_\Phi[(1-\tau)^2]\big). \tag{39b}$$

Substituting (39b) and (38c) into (14a) yields the variance of the stochastic Π-risk. □

E. Proof of Theorem V.4

Proof. Let us obtain the statistics $(\mu_{\Sigma,k}, \sigma^2_{\Sigma,k})$ of the stochastic Σ-risk associated to the updated weapon process Φ_k. This is done by inserting the expression of the extracted process statistics $(\mu_k, \nu_k^{(2)})$, exposed in Proposition V.2, into the statistics given in Theorem IV.1.

We focus first on the mean value. By inserting (24) into (15) we can write

$$\mu_{\Sigma,k} = \int d(x)\tau(x)\mu_k^\phi(x)\mathrm{d}x + \int d(x)\tau(x)\sum_{1\le i\le m}\frac{\mu_k^{z_i}(x)}{F_k^{z_i}[1]+\mu_k^{\mathrm{fa}}(z_i)}\mathrm{d}x. \tag{40}$$

Bringing the sum outside of the integral then yields the desired result.

We focus next on the variance. Next, inserting (24) and (25) into (16) yields

$$\sigma^2_{\Sigma,k} = S_1 - S_2 + S_3, \tag{41}$$

where

$$S_1 = \int d(x)^2\tau(x)^2\mu_k^\phi(x)\mathrm{d}x + \int d(x)^2\tau(x)^2\sum_{1\le i\le m}\frac{\mu_k^{z_i}(x)}{F_k^{z_i}[1]+\mu_k^{\mathrm{fa}}(z_i)}\mathrm{d}x,$$
$$S_2 = \int d(x)\tau(x)d(\bar{x})\tau(\bar{x})\mu_k^\phi(x)\mu_k^\phi(\bar{x})\mathrm{d}(x,\bar{x}) + \int d(x)\tau(x)d(\bar{x})\tau(\bar{x})\mu_k^\phi(x)\sum_{1\le i\le m}\frac{\mu_k^{z_i}(\bar{x})}{F_k^{z_i}[1]+\mu_k^{\mathrm{fa}}(z_i)}\mathrm{d}(x,\bar{x}) + \int d(x)\tau(x)d(\bar{x})\tau(\bar{x})$$

$$\times \sum_{1\leq i,j\leq m} \frac{\mu_k^{z_i}(x)}{F_k^{z_i}[1]+\mu_k^{\mathrm{fa}}(z_i)} \frac{\mu_k^{z_j}(x)}{F_k^{z_j}[1]+\mu_k^{\mathrm{fa}}(z_j)} \mathrm{d}(x,\bar{x}),$$

$$\begin{aligned} S_3 = &\int d(x)\tau(x)d(\bar{x})\tau(\bar{x})\mu_k^{\phi}(x)\mu_k^{\phi}(\bar{x})\mathrm{d}(x,\bar{x}) \\ &+ 2\int d(x)\tau(x)d(\bar{x})\tau(\bar{x})\mu_k^{\phi}(x) \sum_{1\leq i\leq m} \frac{\mu_k^{z_i}(x)}{F_k^{z_i}[1]+\mu_k^{\mathrm{fa}}(z_i)} \mathrm{d}(x,\bar{x}) \\ &+ \int d(x)\tau(x)d(\bar{x})\tau(\bar{x}) \\ &\quad \times \sum_{1\leq i,j\leq m}^{\neq} \frac{\mu_k^{z_i}(x)}{F_k^{z_i}[1]+\mu_k^{\mathrm{fa}}(z_i)} \frac{\mu_k^{z_j}(x)}{F_k^{z_j}[1]+\mu_k^{\mathrm{fa}}(z_j)} \mathrm{d}(x,\bar{x}). \end{aligned}$$

This simplifies to

$$\begin{aligned} \sigma^2_{\Sigma,k} = &\int d(x)^2\tau(x)^2\mu_k^{\phi}(x)\mathrm{d}x \\ &+ \int d(x)^2\tau(x)^2 \sum_{1\leq i\leq m} \frac{\mu_k^{z_i}(x)}{F_k^{z_i}[1]+\mu_k^{\mathrm{fa}}(z_i)} \mathrm{d}x \\ &- \int d(x)\tau(x)d(\bar{x})\tau(\bar{x}) \\ &\quad \times \sum_{1\leq i\leq m} \frac{\mu_k^{z_i}(x)}{F_k^{z_i}[1]+\mu_k^{\mathrm{fa}}(z_i)} \frac{\mu_k^{z_i}(x)}{F_k^{z_i}[1]+\mu_k^{\mathrm{fa}}(z_i)} \mathrm{d}(x,\bar{x}). \end{aligned} \tag{42}$$

Substituting (22) and (23) into (42) yields the desired result. □

ACKNOWLEDGMENTS

The authors would like to thank Yvan Petillot at Heriot-Watt University, Paul Thomas at Dstl, and Isabel Schlangen at Fraunhofer FKIE. The authors also wish to thank Roy Streit for drawing their attention to the interesting work of Bakut and Ivanchuk.

REFERENCES

[1] Liggins II, M., Hall, D., and Llinas, J., *Handbook of multisensor data fusion: theory and practice*. CRC press, 2017.

[2] Roy, J., Paradis, S., and Allouche, M., "Threat evaluation for impact assessment in situation analysis systems," in *Signal processing, sensor fusion, and target recognition XI*, vol. 4729, pp. 329–341, International Society for Optics and Photonics, 2002.

[3] Erlandsson, T. and Niklasson, L., "Automatic evaluation of air mission routes with respect to combat survival," *Information Fusion*, vol. 20, pp. 88–98, 2014.

[4] Kontorov, D. S. and Golubev-Novozhilov, U. S., *Vvedenie v radiolokatsionnuyu sistemoteckniku (Introduction to Radar System Engineering), in Russian*. Sovietskoye Radio, 1971.

[5] Tuzlukov, V., *Signal processing in radar systems*. CRC Press, 2016.

[6] Bolderheij, F., *Mission-driven sensor management: analysis, design, implementation and simulation*. PhD thesis, Delft University of Technology, 2007.

[7] Johansson, F., *Evaluating the performance of TEWA systems*. PhD thesis, Örebro universitet, 2010.

[8] Clark, D. E., "Stochastic Multi-Object Guidance Laws for Interception and Rendezvous Problems," *IEEE Trans. Automatic Control, in print*, 2021.

[9] Lucas, T. W., "Damage functions and estimates of fratricide and collateral damage," *Naval Research Logistics (NRL)*, vol. 50, no. 4, pp. 306–321, 2003.

[10] Hoffman, J. R., Sorensen, E., Stelzig, C. A., Mahler, R. P., El-Fallah, A. I., and Alford, M. G., "Scientific performance estimation of robustness and threat," in *Signal Processing, Sensor Fusion, and Target Recognition XI*, vol. 4729, pp. 248–259, International Society for Optics and Photonics, 2002.

[11] Bakut, P. A. and Ivanchuk, N. A., "Calculation of the a posteriori characteristics of the flow of resolved objects," *Engineering Cybernetics*, vol. 14, no. 6, pp. 148–156, 1976.

[12] Mahler, R. P., "Multitarget Bayes filtering via first-order multitarget moments," *IEEE Transactions on Aerospace and Electronic systems*, vol. 39, no. 4, pp. 1152–1178, 2003.

[13] Schlangen, I., Delande, E. D., Houssineau, J., and Clark, D. E., "A Second-Order PHD Filter With Mean and Variance in Target Number," *IEEE Transactions on Signal Processing*, vol. 66, pp. 48–63, Jan 2018.

[14] De Melo, F. E. and Maskell, S., "A CPHD Approximation Based on a Discrete-Gamma Cardinality Model," *IEEE Transactions on Signal Processing*, vol. 67, no. 2, pp. 336–350, 2019.

[15] Williams, J. L., "Marginal multi-Bernoulli filters: RFS derivation of MHT, JIPDA, and association-based MeMBer," *IEEE Transactions on Aerospace and Electronic Systems*, vol. 51, no. 3, pp. 1664–1687, 2015.

[16] Brekke, E. and Chitre, M., "Relationship between finite set statistics and the multiple hypothesis tracker," *IEEE Transactions on Aerospace and Electronic Systems*, vol. 54, no. 4, pp. 1902–1917, 2018.

[17] Streit, R., Degen, C., and Koch, W., "The pointillist family of multitarget tracking filters," *arXiv preprint arXiv:1505.08000*, 2015.

[18] Helldin, T. and Falkman, G., "Human-centred automation of threat evaluation in future fighter aircraft," in *Proceedings of the 6th. Workshop in Sensor data Fusion: Trends, Solutions, Applications*, 2011.

[19] Katsilieris, F., Driessen, H., and Yarovoy, A., "Radar resource management for improved situational awareness," in *Radar Conference (Radar), 2014 International*, pp. 1–6, IEEE, 2014.

[20] Yang, C., Kaplan, L., and Blasch, E., "Performance measures of covariance and information matrices in resource management for target state estimation," *IEEE Transactions on Aerospace and Electronic Systems*, vol. 48, no. 3, pp. 2594–2613, 2012.

[21] Zwaga, J. and Driessen, H., "Tracking performance constrained MFR parameter control: applying constraints on prediction accuracy," in *Information Fusion, 2005 8th International Conference on*, vol. 1, pp. 6–pp, IEEE, 2005.

[22] Kalandros, M., "Covariance control for multisensor systems," *IEEE Transactions on Aerospace and Electronic Systems*, vol. 38, no. 4, pp. 1138–1157, 2002.

[23] Chepuri, S. P. and Leus, G., "Sparsity-promoting sensor selection for non-linear measurement models," *IEEE Transactions on Signal Processing*, vol. 63, no. 3, pp. 684–698, 2014.

[24] Johansson, F. and Falkman, G., "A Bayesian network approach to threat evaluation with application to an air defense scenario," in *Information Fusion, 2008 11th International Conference on*, pp. 1–7, IEEE, 2008.

[25] Little, E. G. and Rogova, G. L., "An ontological analysis of threat and vulnerability," in *Information Fusion, 2006 9th International Conference on*, pp. 1–8, IEEE, 2006.

[26] Guerriero, M., Svensson, L., Svensson, D., and Willett, P., "Shooting two birds with two bullets: How to find minimum mean OSPA estimates," in *2010 13th International Conference on Information Fusion*, pp. 1–8, IEEE, 2010.

[27] Papageorgiou, D. and Raykin, M., "A risk-based approach to sensor resource management," in *Advances in Cooperative Control and Optimization*, pp. 129–144, Springer, 2007.

[28] Angley, D., Ristic, B., Moran, W., and Himed, B., "Search for targets in a risky environment using multi-objective optimisation," *IET Radar, Sonar & Navigation*, vol. 13, no. 1, pp. 123–127, 2018.

[29] Witkowski, M., White, G., Louvieris, P., Gorbil, G., Gelenbe, E., and Dodd, L., "High-level information fusion and mission planning in highly anisotropic threat spaces," in *11th International Conference on Information Fusion, 2008*, pp. 1–8, IEEE, 2008.

[30] Narykov, A., Delande, E., Clark, D., Thomas, P., and Petillot, Y., "Second-order statistics for threat assessment with the PHD filter," in *2017 Sensor Signal Processing for defence Conference (SSPD)*, IEEE, Dec 2017.

[31] Horrey, W. J., Wickens, C. D., Strauss, R., Kirlik, A., and Stewart, T. R., "Supporting situation assessment through attention guidance and diagnostic aiding: The benefits and costs of display enhancement on judgment skill," *Adaptive perspectives on human technology interaction: Methods and models for cognitive engineering and human-computer interaction*, pp. 55–70, 2006.

[32] Stoyan, D., Kendall, W. S., and Mecke, J., *Stochastic geometry and its applications*. John Wiley & Sons, 1995.

[33] Daley, D. J. and Vere-Jones, D., *An introduction to the theory of point processes. Volume I: Elementary Theory and Methods*. Springer Science & Business Media, 2007.

[34] Delande, E., Üney, M., Houssineau, J., and Clark, D., "Regional variance for multi-object filtering," *IEEE Transactions on Signal Processing*, vol. 62, pp. 3415–3428, July 2014.
[35] Mahler, R. P., "Target preference in multitarget sensor management: A unified approach," in *Defense and Security*, pp. 210–221, International Society for Optics and Photonics, 2004.
[36] Panicker, S., Gostar, A. K., Bab-Haidashar, A., and Hoseinnezhad, R., "Sensor control for selective object tracking using labeled multi-Bernoulli filter," in *2018 21st International Conference on Information Fusion (FUSION)*, pp. 2218–2224, IEEE, 2018.
[37] Vo, B.-N., Singh, S., and Doucet, A., "Sequential Monte Carlo methods for multitarget filtering with random finite sets," *IEEE Transactions on Aerospace and electronic systems*, vol. 41, no. 4, pp. 1224–1245, 2005.
[38] Clark, D. E. and de Melo, F., "A linear-complexity second-order multi-object filter via factorial cumulants," in *2018 21st International Conference on Information Fusion (FUSION)*, pp. 1250–1259, IEEE, 2018.
[39] Ditzel, M., Kester, L., van den Broek, S., and van Rijn, M., "Cross-layer utility-based system optimization," in *Proceedings of the 16th International Conference on Information Fusion*, pp. 507–514, IEEE, 2013.
[40] Katsilieris, F., Driessen, H., and Yarovoy, A., "Threat-based sensor management for target tracking," *IEEE Transactions on Aerospace and Electronic Systems*, vol. 51, no. 4, pp. 2772–2785, 2015.
[41] Benavoli, A., Ristic, B., Farina, A., Oxenham, M., and Chisci, L., "An application of evidential networks to threat assessment," *IEEE Transactions on Aerospace and Electronic Systems*, vol. 45, pp. 620–639, April 2009.

Alexey Narykov received a Ph.D. in Electrical Engineering in 2020 jointly from Heriot-Watt University and the University of Edinburgh, Scotland. Previously, from 2011 to 2014 he carried out research on radar resource management at Delft University of Technology, the Netherlands. Since 2020 he is a postdoctoral research associate in the University of Liverpool, England, where he works on Bayesian localisation in the underwater environment. His principle research interest lies with adapting Bayesian filtering algorithms to practical applications.

Emmanuel Delande is a Space surveillance engineer with the Centre National d'Études Spatiales (CNES) in Toulouse (France). He holds a Ph.D. in signal processing from the École Centrale de Lille (Lille, France). His research interests are in the modelling of Bayesian estimation algorithms for target tracking applications, in the context of space surveillance awareness. His main focus is on the development of multi-object filtering solutions with point processes, and the representation of uncertainty with non-probabilistic formulations.

Daniel Clark is Head of the TIPIC group in the SAMOVAR research laboratory at Telecom Sud-Paris, Institut Polytechnique Paris in France. His research interests are in the development of the theory and applications of multi-object estimation algorithms for sensor fusion problems. He has led a range of projects spanning theoretical algorithm development to practical deployment. He was elected Fellow of the Royal Aeronautical Society, the Institute of Engineering and Technology, and the Institute of Mathematics and its applications in 2021.

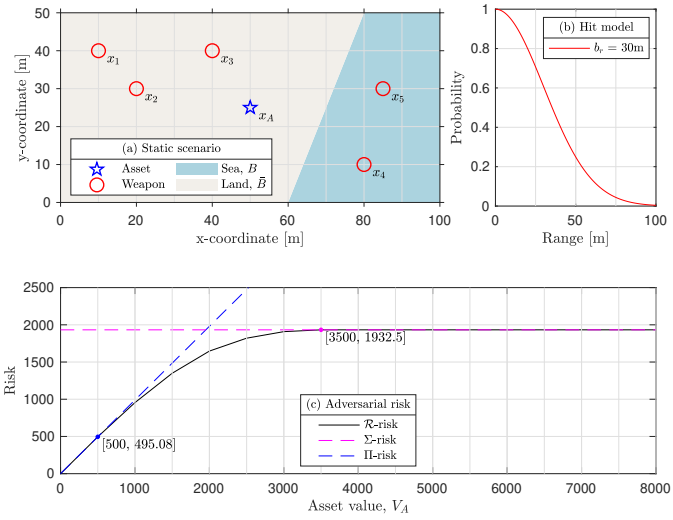

Fig. 1. Evaluation of adversarial risk: (a) 2D representation of the scenario, where a single asset is juxtaposed with three land-based and two sea-based adversaries; (b) the model of hit probability as a function of range between the asset and an adversary; (c) adversarial risk as a function of the asset value.

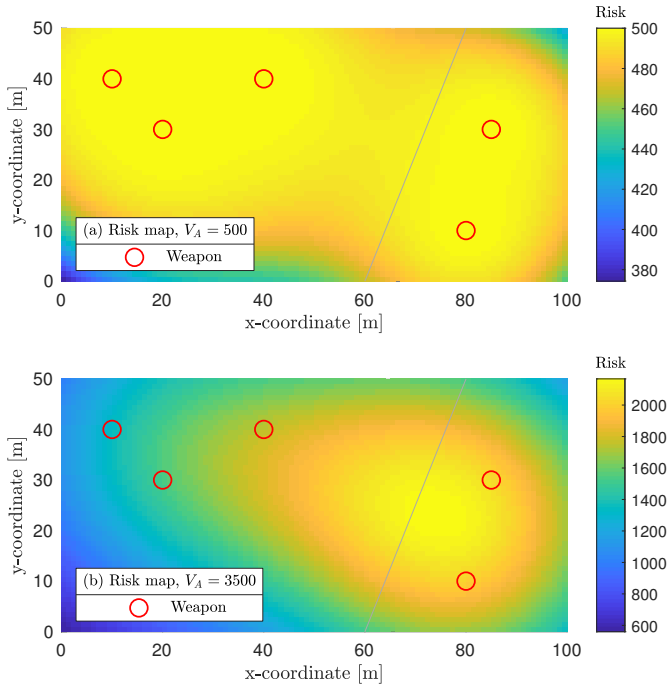

Fig. 2. Risk maps produced by freely moving the asset location in the 2D plane. The asset value is set to: (a) $V_A = 500$; (b) $V_A = 3500$. The difference in shape of the *riskier* areas is due to the interaction between the asset value and the weapon damaging capacities. Note that the absolute values of adversarial risk are presented using different scales.

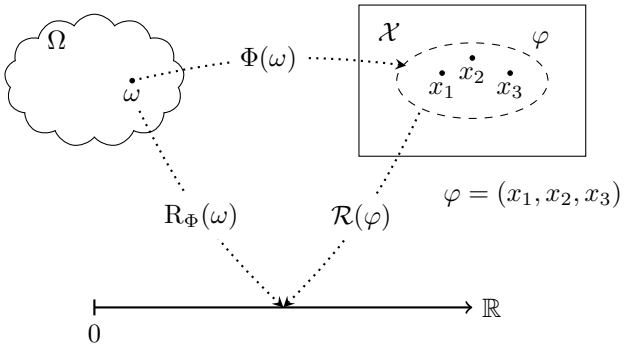

Fig. 3. Spatial point process and adversarial risk. The point process Φ maps an element ω in the sample space Ω into a sequence of points φ in the state space $\mathcal{X}$. $\mathcal{R}$ evaluates the adversarial risk for any given sequence φ. Allowing the sequence of points to vary with the realisation of the point process Φ leads to the construction of a *stochastic* adversarial risk, described by the real-valued random variable R_Φ.

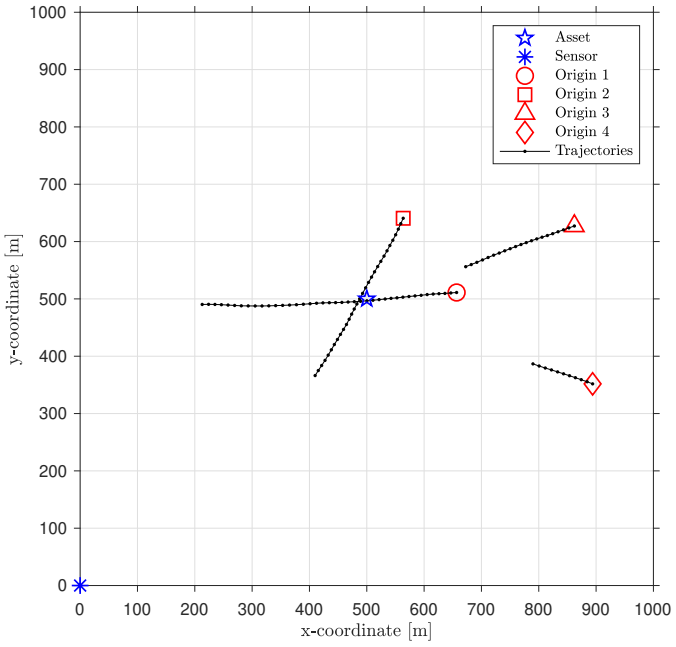

Fig. 4. Ground truth: position plots of 4 weapon tracks superimposed over 50 time steps. The asset is located in $[500, 500]^T$ m, and the sensor is located at the origin.

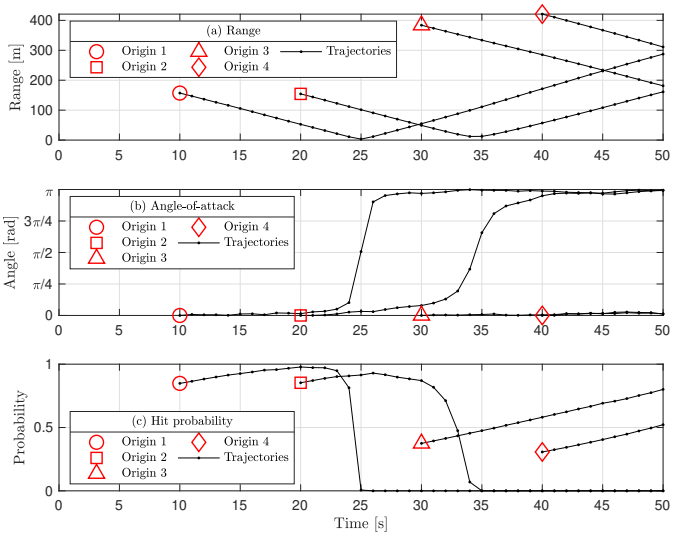

Fig. 5. Ground truth: plots of relative range, angles and corresponding hit probabilities for the 4 true weapon tracks against time, showing the different start times.

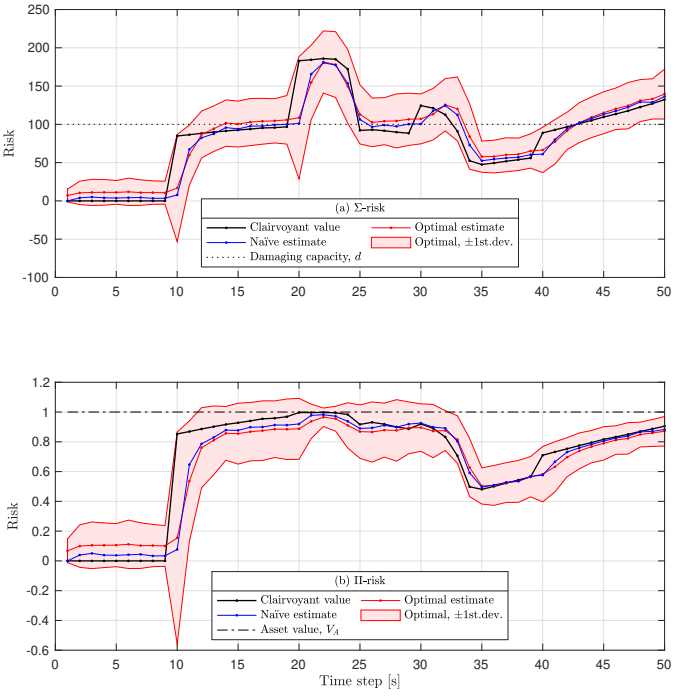

Fig. 6. Application of the SMC-PHD intensity filter for estimation of adversarial risk: (a) Σ-risk with uniform $d_A = 100$, and (b) Π-risk with $V_A = 1$; from data synthesized using a sensor with $p_\mathrm{d} = 0.95$. Clairvoyant risk values (solid black line) are computed using the ground truth and presented next to their estimated values. In contrast to naïve estimates (solid blue line), the optimal estimates (solid red line) are additionally equipped with indicators of their quality (depicted as an interval of ± 1 standard deviation, i.e. square root of variance). The results are averaged over 500 Monte Carlo runs.

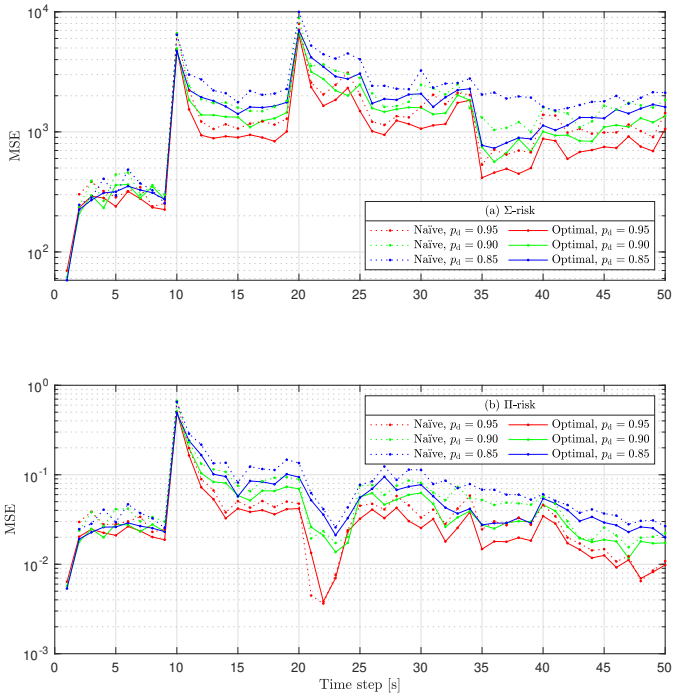

Fig. 7. Mean squared error describing the performance of algorithms estimating: (a) Σ-risk with uniform $d = 100$, and (b) Π-risk with $V_A = 1$; under varying probabilities of detection p_{d}. The MSE values are demonstrated for the naïve (dotted lines) and optimal (solid lines) algorithms. The results are averaged over 500 Monte Carlo runs.

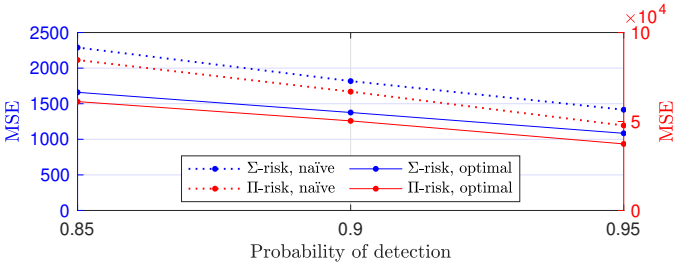

Fig. 8. Average MSE performance (over the total length of scenario) for the naïve (dotted line) and optimal (solid line) approaches. The results are presented using two different scales: the left scale (in blue) for Σ-risk, and the right scale (in red) for Π-risk.